PHYSICAL REVIEW A VOLUME 45, NUMBER 3 1 FEBRUARY 1992

Convoy-electron emission in 20–100-keV grazing proton bombardment of Cu(100)

E. A. Sánchez, M. L. Martiarena, O. Grizzi, and V. H. Ponce
Centro Atómico Bariloche, Comisión Nacional de Energía Atómica, 8400 San Carlos de Bariloche, Río Negro, Argentina
(Received 19 March 1991; revised manuscript received 1 October 1991)

We investigate the convoy-electron (CE) emission produced during grazing bombardment of a Cu(100) surface with 20–100-keV protons. At 0.5° of incidence the CE peak measured at projectile energies below 50 keV along the direction of specular reflection of the ions has a width and shape similar to that of the CE peak corresponding to H^+-He collisions and is considerably narrower than that observed in transmission through thin foils. This finding shows that CE's are mainly subjected to the Coulomb potential of the scattered ion when the velocity resolutions are high enough to localize electron states close to the ion velocity. A strong variation of the CE peak shape with the projectile incidence angle was also observed. This result is discussed in terms of a calculation that takes into account the angular distribution of the reflected ions.

PACS number(s): 79.20.Nc, 79.20.Rf

Ions hitting flat surfaces at grazing angles reflect specularly with little penetration when the incidence angle is sufficiently small. At directions of observation around that of the reflected ions, the energy distribution of the ejected electrons is dominated by a cusp structure superimposed on a relatively small background. This cusp peak appears at an electron velocity which is close to the reflected projectile velocity and is usually assigned to convoy electrons (CE) of the scattered ions [1–3].

The shape and intensity of the CE peak are determined by three processes: (i) reflection of the ions at the surface, (ii) excitation of electrons either from bound states of the projectile or surface states to continuum states centered on the moving ion, and (iii) the final-state interaction between the excited electron, the projectile, and surface electrons. The importance of each process may vary considerably with the type of projectile, surface, angle of incidence, and bombarding energy. For example, the angular distribution of the reflected ions and mechanisms for electron excitation are different for a well-ordered single crystal and an evaporated polycrystal, where violent collisions are possible for any angle of incidence. High-energy projectiles, around 1 MeV/amu, generate a polarization of surface electrons that is far from adiabatic with the motion of the scattered projectiles. The resulting spatial and velocity distributions of the excited surface electrons are therefore different from those of electrons excited by low-energy projectiles. These initial distributions will determine the population of bound and continuum states of the projectile. For highly charged ions [4], the strong image polarization modifies the pure Coulombic final-state interaction between projectile and CE, affecting both the shape and the velocity of the CE, while for H^+ ions, the effect of the projectile image charge can be partially compensated by the electron self-energy [5]. In this way, the energy and charge of the projectiles can be chosen so that a particular interaction mechanism is enhanced.

The main features observed in recent experiments [1–6] performed in the energy range of 0.05–1 MeV/amu are (a) the CE peak measured in specular reflection of ions at surfaces is broader than that of beam-foil experiments and (b) for highly charged projectiles [4], the CE peak is shifted to a velocity higher than that of the projectile. These effects have been attributed [2–4] to a deviation from the Coulombic final-state interaction between the reflected projectile and CE caused by the dynamic image potential of the projectile.

In the present work we report measurements and a preliminary calculation of CE spectra obtained by H^+ grazing bombardment of a Cu single crystal. In the energy range of our experiment, 20–100 keV, the proton-surface interaction time is longer than in previous measurements, so surface electrons react quasiadiabatically to the grazing ion, and postcollisional interactions with the surface should become stronger. In order to investigate angular regions around that of specular reflection, where different types of postcollisional interactions could be present, spectra with high angular resolution were measured as a function of the energy and incidence angle of the projectile. Under these conditions, CE spectra obtained for specular reflection are compared with those obtained in transmission through thin foils and gaseous targets.

The measurements were performed in an UHV chamber equipped with standard facilities for sample cleaning and Auger analysis. The sample, a Cu(100) single crystal disk of 6 mm diameter, was polished with alumina of 0.05 μm and then cleaned by annealing at $\simeq$1100 K by electron bombardment from the back of the sample. The only contaminant detected by Auger spectroscopy was sulfur in a small amount. A proton beam was produced in a radio-frequency source, then accelerated to 20–100 keV, mass-analyzed by a magnet, and finally collimated to a spot of 0.5 mm diameter with angular divergence of 0.1°. Electrons ejected in a cone of half-angle $\theta_0 = 0.7°$ were energy analyzed with a resolution of 1% by a custom-made [7] rotatable cylindrical mirror analyzer. The spectra were corrected, taking into account the transmission of the electron energy analyzer.

Figure 1 shows electron spectra obtained for two projec-

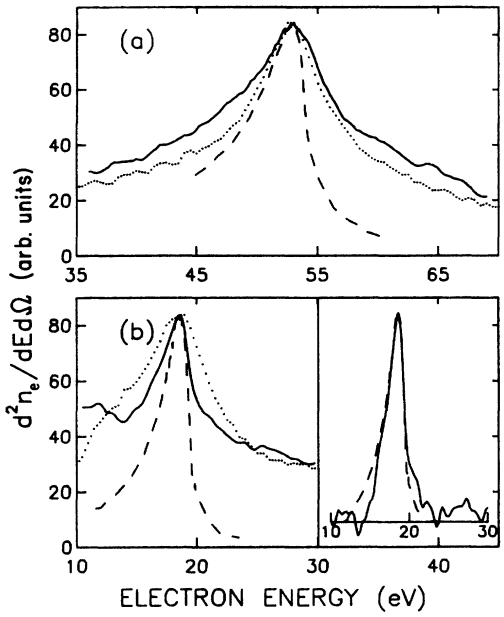

FIG. 1. (a) Energy distributions of electrons ejected in specular reflection of 100-keV H^+ from a Cu single crystal (——), transmission through Al foil (····), and H^+-He collisions (---). The proton energy in the foil experiment has been adjusted to match the corresponding CE energy to that of the reflection case. (b) Same as (a) for a projectile energy of 35 keV. The inset shows the Cu and He spectra after background subtraction.

tile energies, 100 and 35 keV, in (1) specular reflection of H^+ from Cu(100) with incidence angle $\varphi=0.5°$, (2) transmission of H^+ through an Al foil of 560 Å thickness, and (3) H^+-He collisions. The spectra corresponding to reflection and transmission were taken in the same chamber. According to a numerical simulation of the transmission experiment (TRIM-1990), the projectile energy loss is about 10%, the straggling less than 2% of the initial energy, and the angular dispersion about 1.5°. The gas-phase spectra, taken with similar resolution to that of the present measurements, were provided by Suárez and Meckbach [8].

The spectra shown in Fig. 1(a) are similar to those obtained previously [1,3], with the width of the spectrum under specular observation broader than those of gas-phase and thin foils experiments. For lower proton energy [Fig. 1(b)] the CE peaks obtained in ion-solid experiments are mounted over the secondary-electron distribution, which is negligible for the ion-gas case [9]. For a better comparison between the ion-reflected and the gas-phase electron spectra, the low-energy background has been subtracted by an interpolating function [2,10]. The corresponding spectra are shown in the inset of Fig. 1(b), in which a striking feature is observed: Their widths and overall shapes are very similar. A possible explanation for this feature comes from the following analysis of the collision process: The electron capture (or loss) to the continuum occurs when the ion is close to the surface. This electron outgoing state originates from a finite region around the projectile, where the interaction acting on the initial electron state is strong enough to produce the transition. At a time t well after this process, the relative electron-projectile distance will approximately satisfy the classical relation $r \simeq |\mathbf{v}_e - \mathbf{v}_i| t$, where $\mathbf{v}_e$ and $\mathbf{v}_i$ are the electron and ion velocities, respectively. The final electron distribution is modeled by both the projectile potential and the induced (image) potential due to the surface electron polarization. Their relative influence will depend on the distance of the electron from both potential centers; therefore, the effective post-collision interaction character will tend to be pure Coulombic when $|\mathbf{v}_e - \mathbf{v}_i| \ll v_\perp$ and pure dipolar for $|\mathbf{v}_e - \mathbf{v}_i| \gg v_\perp$, where $v_\perp$ is the component of $\mathbf{v}_i$ normal to the surface. The electron distribution measured along the direction of specular reflection θ_r will depend on the average character of the final electron interaction in the detector resolution volume. The angular aperture θ_0 determines the region of electron velocities covered by the detector: $|\mathbf{v}_e - \mathbf{v}_i| \leq \theta_0 v_\perp / \theta_r$. The present experimental condition is $\theta_0 \lesssim \theta_r$, so we are away from the region of prevailing dipole final interaction ($\theta_0 \gg \theta_r$), and, rather, have a detection of electrons with dominant final Coulombic interaction. Other electron-detector resolutions, such as those used by Winter, Strohmeier, and Burgdörfer [3], may shift the weight to final electron velocities where the dipole interaction is dominant.

The dependence of the electron energy distribution with the incidence angle φ along the specular reflection direction $\theta_r = \varphi$ is shown in Fig. 2 for incident protons of 80 keV. We see that (i) the width of the peak for $\varphi = 2°$ is about twice that of 0.5°, (ii) the asymmetry observed at ow projectile energy is conserved, (iii) within the experinental uncertainties, there is no change in the CE peak energy, and (iv) the secondary-electron background increases with φ. The last point is a consequence of the larger electron escape probability for increasing observation angles and the larger cascade of electrons generated by projectiles impinging on the surface with larger incidence angles. The broadening observed on the CE peaks

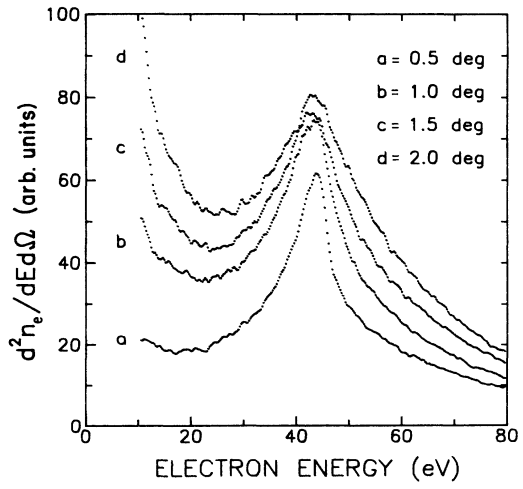

FIG. 2. Energy distribution of electrons emitted during 80-keV H^+ bombardment of a Cu single crystal, measured along the direction of the ion specular reflection for the incidence angle indicated in the figure. Counts are normalized with the fraction of the beam hitting the sample.

with increasing φ cannot be explained as a post-collision interaction effect, since its Coulomb character is enhanced for increasing θ_r, and this will tend to produce sharper peaks. At larger incidence angles, the excitation to continuum states of the projectile can occur closer to the surface, but, according to the experiments of Hasegawa *et al.* [6], this should have little effect on the final peak shape since the observed convoy electrons are generated at distances from the surface larger than 2 Å; excited electrons within that distance from the surface are easily scattered away by collisions with other surface electrons. The broadening could come from the CE transport through the surface electron density that, through elastic and inelastic processes, will widen and asymmetrize the peak. Even though this effect can contribute to the final peak shape, we think that it is not the main cause for the increasing width with angle θ_r, since the path of CE through the region of appreciable surface electron density is inversely proportional to θ_r. Finally, the broadening may originate from the angular and velocity distributions of reflected projectiles, which depend on incidence angle, projectile energy, and surface topography. In order to estimate this, we have performed a preliminary calculation, taking into account the elastic scattering of projectiles from flat surfaces. Inelastic processes, with the corresponding straggling of reflected projectile energy, and effects due to the surface topography, will be considered in a future publication. The CE distribution has been calculated assuming a pure Coulomb final interaction, described by the electron distribution taken from ion-atom collisions and parametrized as [11]

$$f(\mathbf{v}_e,\mathbf{v}_i)=\frac{2\pi}{v'}[B_{00}+B_{10}v'+B_{20}v'^2 + \cos\theta'(B_{01}+B_{11}v'+B_{21}v'^2)]$$

where $v'=|\mathbf{v}_e-\mathbf{v}_i|$ and θ' is the angle formed between $\mathbf{v}'$ and $\mathbf{v}_i$.

The complete angular distribution of the elastically scattered ions $W(\vartheta,\phi)$ was taken from Remizovich, Ryazanov, and Tilinin [12]. Here ϑ and ϕ are the polar and azimuthal angles in the reference system in which the z axis is determined by the intersection of surface and incident plane. This distribution has a maximum at the specular condition and is asymmetric with a tail towards larger reflection angles, as can be observed in the inset in Fig. 3.

The influence of the reflected ion distribution on the CE emission is then evaluated as

$$Q(\mathbf{v}_e)=\int_{-\pi/2}^{\pi/2}\int_0^{\pi/2}\sin(\vartheta)d\vartheta\,d\phi\,W(\vartheta,\phi) \times\int_{C(\mathbf{v}_e)}f(\mathbf{v}'_e,\mathbf{v}_i)d\mathbf{v}'_e\,,$$

where $C(\mathbf{v}_e)$ is the detector resolution volume centered at the observation velocity $\mathbf{v}_e$. Figure 3 shows the calculated electron energy distributions for 80-keV proton bombardment of a Cu sample under the conditions used in the experiment. Even though this simple model cannot reproduce details of the peak shape, it does reproduce the changes observed experimentally in the width. The full

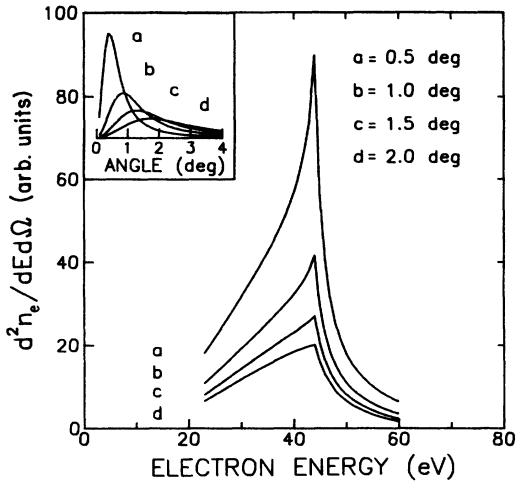

FIG. 3. Energy distribution of electrons calculated for the experimental conditions of Fig. 2. The inset shows the distributions of the reflected projectiles as used in the calculation vs the reflection angle.

width at half maximum (FWHM) obtained from the calculation and experimental spectra after subtraction of the ionization electron background [10] for specular observation were as follows, for $\varphi=\theta_r$:

	FWHM (eV)			
	$\varphi=0.5°$	$\varphi=1.0°$	$\varphi=1.5°$	$\varphi=2.0°$
Calculation	9.4	13.8	17.6	20.1
Experiment	10	14	16	20

The error due to this background subtraction is regarded to be less than 5%. This result shows that at least an important component of the broadening of the CE peaks comes from the angular distribution of the reflected projectiles. The discrepancies observed in the CE yield could come from the fact that for lower observation angles the electrons deviate more easily from their trajectory to the electron detector because of the multiple collisions with the surface electrons.

In summary, we have presented CE peaks measured along the direction of the ion specular reflection from surfaces which are narrow and very similar in shape to CE peaks observed in gas-phase collisions. This shows that the CE measured for energies below 50 keV with small enough ion incidence angle ($\simeq 0.5°$) are mainly subjected to the Coulomb potential of the scattered ion when the analyzer resolutions are precise enough to localize electron states close to the ion velocity. A strong broadening on the CE peak shape was also observed with increasing energy or projectile incidence angle. A simple calculation assuming a pure Coulombic final ion-electron interaction for the particular angular region of the experiment has indicated that the angular distribution of the reflected ions strongly affects the final electron energy distribution. The dependence of the CE peak shape with the observation angle for fixed angle of incidence, the angular resolution and the rugosity of the sample will be discussed in a forthcoming work.

We thank C. Wenger and J. De Pelegrin for their expert technical assistance, W. Meckbach for revision of the manuscript, and we acknowledge partial support by Consejo Nacional de Investigaciones Científicas y Técnicas (CONICET).

[1] L. F. de Ferrariis and R. A. Baragiola, Phys. Rev. A **33**, 4449 (1986).

[2] K. Kimura *et al.*, Nucl. Instrum. Methods Phys. Res. Sect. B **33**, 358 (1988); M. Hasegawa, K. Kimura, and M. Mannami, J. Phys. Soc. Jpn. **57**, 1834 (1988).

[3] H. Winter, P. Strohmeier, and J. Burgdörfer, Phys. Rev. A **39**, 3895 (1989).

[4] A. Koyama *et al.*, Phys. Rev. Lett. **65**, 3156 (1990); T. Iitaka *et al.*, *ibid.* **65**, 3160 (1990).

[5] T. Iitaka *et al.* (unpublished).

[6] M. Hasegawa, T. Uchida, K. Kimura, and M. Mannami, Phys. Lett. A **145**, 182 (1990).

[7] L. F. de Ferrariis, F. Tutzauer, E. A. Sánchez, and R. A. Baragiola, Nucl. Instrum. Methods Phys. Res. Sect. A **281**, 43 (1989).

[8] S. Suárez and W. Meckbach (private communication).

[9] Y. Yamazaki, in *High-Energy Ion-Atom Collisions,* edited by D. Berenyi and G. Hock, Lecture Notes in Physics Vol. 294 (Springer, Berlin, 1988), p. 321.

[10] H. Rothard *et al.*, J. Phys. C **21**, 5033 (1988); J. Phys. (Paris) Colloq. **48**, C9-215 (1987).

[11] W. Meckbach, L. B. Nemirovsky, and C. R. Garibotti, Phys. Rev. A **24**, 1793 (1981).

[12] V. S. Remizovich, M. I. Ryazanov, and I. S. Tilinin, Zh. Eksp. Teor. Phys. **79**, 448 (1980) [Sov. Phys. JETP **52**, 225 (1980)].